

**ICEWEST-2015 [05<sup>th</sup> - 06<sup>th</sup> Feb 2015]****International Conference on Energy, Water and  
Environmental Science & Technology****PG and Research Department of Chemistry, Presidency College (Autonomous),  
Chennai-600 005, India****Size dependent magnetic properties of BiFeO<sub>3</sub> nanoparticles:  
A multifunctional material for saving energy****S.V. Vijayasundaram and R. Kanagadurai****Department of Physics, Presidency College, Chennai – 600 005, India.**

**Abstract :** BiFeO<sub>3</sub> (BFO) is a unique room temperature multiferroic material with high ferroelectric Curie temperature ( $T_C$ ) and Néel temperature ( $T_N$ ). BFO is gaining much attention due to its technological and fundamental importance for the future electronic devices. Single-phase BFO nanoparticles of size about 25 – 70 nm were synthesized using acetic acid as chelating agent through wet chemical sol-gel process with ethylene glycol. The synthesized nanoparticles were subjected to FTIR, XRD, HRTEM and VSM analyses. The observed powder X-ray diffraction patterns confirm the single-phase of BFO nanomaterials. The size of the polycrystalline particles, found from TEM, is comparable with the spin-periodicity of BFO and the key for unlocking the latent ferromagnetism in BFO. The correlation between the size and magnetic property of the samples is well established by studying the room temperature M-H loops.

**Introduction**

In recent years, magnetoelectric multiferroics have attracted considerable attention due to their intriguing properties and potential applications. The coupling between the magnetic and electronic structures in multiferroics, namely, magnetoelectric effect, could provide an additional degree of freedom in device design, which is more attracting than the ferroelectricity or magnetism itself. Of all multiferroic materials studied recently, BFO is considered as a representative multiferroic material with  $T_C$  around 830 °C and  $T_N$  around 370 °C<sup>1</sup>. It has a rhombohedrally distorted perovskite structure with the space group  $R3c^2$ . Its G-type antiferromagnetism due to the local spin ordering of Fe<sup>3+</sup> forms a cycloidal spiral spin structure with a spin-periodicity of 62 nm<sup>3,4</sup>. This helimagnetic structure results in almost zero macroscopic magnetization and thus studying the properties of BFO particles of size less than 62 nm is important for enhanced ferromagnetism and potentially enhanced magnetoelectric coupling which are promising for multifunctional smart materials<sup>5</sup>.

**Experimental****Material synthesis**

BFO powders were prepared through modified Pechini type sol-gel method. Ultrapure Bi(NO<sub>3</sub>)<sub>3</sub>.5H<sub>2</sub>O and Fe(NO<sub>3</sub>)<sub>3</sub>.9H<sub>2</sub>O in stoichiometric proportions (1:1 molar ratio) were dissolved in 2-methoxyethanol to

prepare a precursor solution. Acetic acid and ethylene glycol (EG)(1:1 molar ratio to the metal cations) were added as a chelating agent and polymerizing agent respectively in the precursor solution. The solution was continuously stirred on a hot plate at 90°C to obtain a gel. The gel was dried and ground into fine powders. These “as-synthesized powders” were calcined at various temperatures and time such as 500°C for 1 h, 2 h, 3h, 4 h and 550 °C for 1 h, 2h, 3h, 4h and named as S1, S2, S3, S4, S5, S6, S7 and S8 respectively.

### Characterizations

The phases and structures of the calcined specimens (S1-S8) were examined by X-ray diffraction (XRD) using a Rigaku Miniflex diffractometer with Cu K $\alpha$  radiation ( $\lambda = 1.5406 \text{ \AA}$ ). The samples were made into pellets with KBr for FTIR studies and the spectra were recorded in the range 450 – 4000  $\text{cm}^{-1}$  using Perkin Elmer spectrometer. Micro structural properties of the samples were examined by TECHNAI G<sup>2</sup>HR Transmission Electron Microscope. Room temperature magnetic properties of the samples in maximum applied fields of 16 kOe were measured using a Lakeshore 7407 vibrating sample magnetometer (VSM).

## Results and discussion

### FTIR analysis

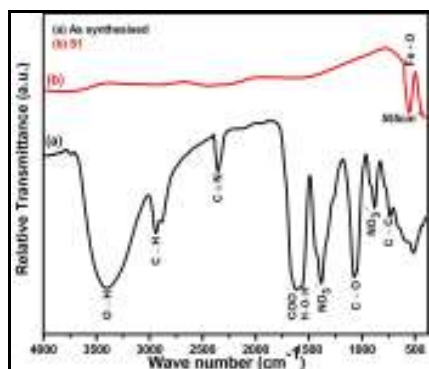


Fig.1. FTIR absorption spectra of (a) as-synthesized sample of BFO, (b) S1

The figure 1 (a) shows the FTIR spectra of as-synthesized BFO powders. The wide peaks located around 3407  $\text{cm}^{-1}$  in the patterns (a) is assigned to the stretching vibrations of hydroxyl (OH) group<sup>6</sup>, while a band at 1574  $\text{cm}^{-1}$  corresponds to the bending vibrations of H-O-H<sup>7</sup>. The peak at 2942  $\text{cm}^{-1}$  is assigned to C-H symmetric stretching<sup>8</sup>. The peaks observed at 1628, 1069 and 737  $\text{cm}^{-1}$  are attributed to the stretching vibrations of C=O, C-O and C-C in acetic acid respectively<sup>9</sup>. The bands at 882, and 1383  $\text{cm}^{-1}$  are ascribed to the traces of trapped  $\text{NO}_3^-$  ions in the samples<sup>8</sup>. On the other hand, nitrile formation is observed at 2354  $\text{cm}^{-1}$ . Fig. 1 (b) illustrates the spectrum of S1 in which the absorption band at 555  $\text{cm}^{-1}$  is the characteristic for the Fe-O stretching vibrations of octahedral  $\text{FeO}_6$  group in the perovskite compounds<sup>10</sup>. Evidently, the disappearance of all the organic peaks in the spectrum reveals that a well-crystalline BFO phase is formed in the sample S1.

### Structural Analysis

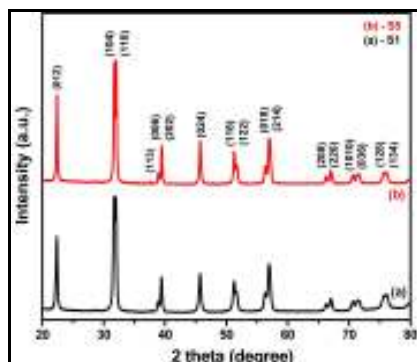
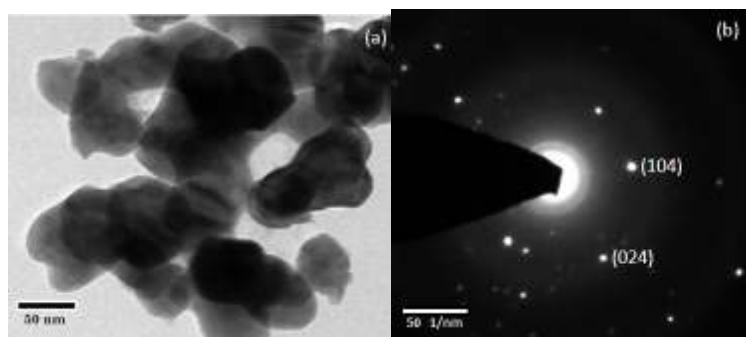


Fig.2. Powder XRD patterns of the samples S1 and S5

The figure 2 represents the powder XRD patterns of the samples S1 and S5. The diffraction peaks emerged in both the patterns are strong and sharp, indicating well crystallization of BFO starting from the temperature 500 °C. The patterns exhibit a distorted perovskite structure that belongs to the  $R3c$  space group with lattice parameters of  $a = b = 5.5876 \text{ \AA}$   $c = 13.8670 \text{ \AA}$ . These results are in a good agreement with the ICDD data #96-100-1091<sup>11</sup>. Secondary phases were not detected in both the XRD patterns, which indicate that the discussed properties are solely exhibited by the single-phase BFO nanoparticles. From the XRD patterns, the average crystallite sizes of the BFO were calculated using the Scherrer equation. The estimated grain sizes were 32, and 40 nm for the samples S1 and S5 respectively.

### HRTEM Analysis



**Fig.3.** HR TEM images of the sample S1 (a) macroscopic view (b) SAED Pattern

The figure 3 (a) and (b) display the HRTEM images. From the image (a), it is seen that the particles are oblate spheroidal and agglomerated. Polycrystalline nature of the sample is confirmed from the selected area electron diffraction (SAED) pattern shown in the image (b). The particle size distribution was calculated for the images taken and fitted using Gaussian function, which reveals that the average diameter of the nanoparticles is  $65.2 \pm 11 \text{ nm}$ . It is in reasonable agreement with the crystallite size estimated from Fig. 2.

### Magnetic Analysis

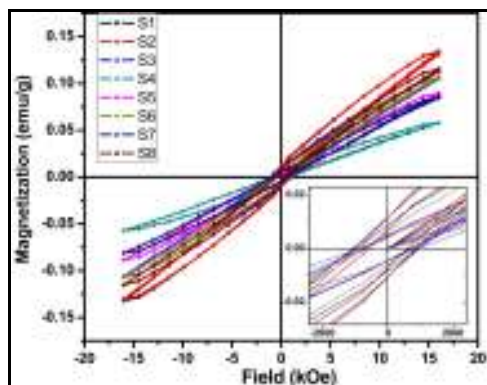


**Fig.4.** Magnetic hysteresis loop obtained for various calcined samples of BFO at RT.

**Table1.** Magnetic data from the Hysteresis loops of various BFO samples taken at room temperature (RT).

Sample Code	Hci(Oe)	Ms (emu/g)	Retentivity (emu/g)
S1	1039.59	0.13	0.011
S2	947.16	0.13	0.011
S3	979.59	0.11	0.009
S4	889.92	0.06	0.005
S5	747.65	0.09	0.004
S6	749.20	0.11	0.006
S7	760.04	0.08	0.005
S8	597.78	0.12	0.007

The figure 4 shows the M-H loops recorded at room temperature for the samples S1-S8. The table 1 lists the magnetic properties of the corresponding samples. In general, M vs H relationship of BFO is linear. However, all the samples (S1-S8) exhibit the distinct nonlinear M-H loops with obvious coercivities, which demonstrate a weak ferromagnetic order of the samples. In general, the secondary phases such as  $\text{Fe}_3\text{O}_4$ , and  $\text{Bi}_2\text{Fe}_4\text{O}_9$ , could be responsible for this kind of weak ferromagnetism<sup>12</sup>, but it has been very well established from our XRD studies (Fig.2 (a) & (b)) that the samples have single-phase BFO and hence the presence of secondary phases are ruled out. Moreover, the presence of secondary phases saturate M-H loop at lower field, but the M-H loops recorded up to 16 kOe are not saturated for all the samples, thereby again discounting the secondary phases as being responsible for the observed weak ferromagnetism in the samples<sup>12</sup>. Thus the observed ferromagnetic property is firstly, due to non-exact compensation of two magnetic sublattices and secondly, considering the particle size, due to the suppression of cycloidal spin structure of phase pure BFO nanoparticles<sup>13,14</sup>. The inset of Fig.4 shows the coercivities of the samples. With the trend observed from the hysteresis loops and the corresponding obtained data given in the table 1, it is clear that the size plays a key role in the magnetic properties of BFO nanoparticles.

## Conclusions

Nearly spherical and phase pure BFO nanoparticles, having an average size of 65 nm, were successfully synthesized using acetic acid as chelating agent through modified Pechini sol-gel process. The single-phase from XRD results accompanied with FTIR and the comparable particle size to cycloidal spin periodicity of 62nm from TEM micrograph confirmed that the uncompensated spin moments on the surface and the breaking of the spin cycloid are the reasons for the observed weak ferromagnetism at room temperature in the calcined BFO samples. The estimated crystallite sizes from the Scherrer equation demonstrate that the particle size increases as the temperature or duration of calcination increases. The observed M-H loops for various calcined samples demonstrate that the  $M_s$  decreases with the increase in particle size. Eventually, increase in calcination time or temperature, increases the size of particles, which in turn decreases the magnetic properties such as  $M_s$ ,  $H_{ci}$  and  $M_r$ . Of all the samples, S1 can be used for applications as it exhibits the best magnetic properties. Thus BFO of size less than 60 nm will be useful for the application of room temperature nano multifunctional energy devices.

## Acknowledgements

S.V.VandR.K thank the University Grants Commission (UGC), Government of India for the financial support through the Major Research Project (MRP) F.No.42-827/2013(SR).

## References

1. Ramesh R, Spaldin NA. Multiferroics: Progress and prospects in thin films, *Nat. Mater.*, 2007, 6 : 21–29.
2. Moreau JM, Michel C, Gerson R, James WJ. Ferroelectric  $\text{BiFeO}_3$  X-Ray and Neutron Diffraction Study. *J. Phys. Chem. Solids.*, 1971, 32 : 1315–1320.
3. Fischer P, Polomska M, Sosnowska I, Szymanski M. Temperature dependence of the crystal and magnetic structures of  $\text{BiFeO}_3$ , *J. Phys. C: Solid State Phys.*, 1980, 13 : 1931–1940.
4. Catalan G, Scott JF. Physics and Applications of Bismuth Ferrite. *Adv. Mater.*, 2009, 21: 2463–2485.
5. Xie SH, Li JY, Roger Proksch, Liu YM, Zhou YC, Liu YY, Ou Y, Lan LN, Qiao Y. Nanocrystalline multiferroic  $\text{BiFeO}_3$  ultrafine fibers by sol-gel based electrospinning, *Appl. Phys. Lett.*, 2008, 93 : 222904.
6. Shao J, Tao Y, Wang J, Xu C, Wang WG. Investigation of precursors in the preparation of nanostructured  $\text{La}_{0.6}\text{Sr}_{0.4}\text{Co}_{0.2}\text{Fe}_{0.8}\text{O}_{3-\delta}$  via a modified combined complexing method. *J. Alloys Compd.*, 2009, 484 : 263–267.
7. Yang H, Xian T, Wei ZQ, Dai JF, Jiang JL, Feng WJ. Size-controlled synthesis of  $\text{BiFeO}_3$  nanoparticles by a soft-chemistry route. *J. Sol-Gel Sci. Technol.*, 2011, 58 : 238–243.
8. Xian T, Yang H, Shen X, Jiang JL, Wei ZQ, Feng WJ. Preparation of high-quality  $\text{BiFeO}_3$  nanopowders via a polyacrylamide gel route., *J. Alloys Compd.*, 2009, 480: 889–892.
9. Nakanishi K, Solomon PH. Infrared Absorption Spectroscopy, Holden Day, San Francisco, 1977.
10. Rao GVS, Rao CNR, Ferraro JR. Infrared and Electronic Spectra of Rare Earth Perovskites: Ortho-Chromites. Manganites and Ferrites, *Appl. Spectrosc.*, 1970, 24 : 436-445.

11. Moreau JM, Michel C, Gerson R, James WJ. Ferroelectric BiFeO<sub>3</sub> X-Ray and neutron diffraction study. J. Phys. Chem. Solids, 1971, 32 :1315-1320.
12. Bernardo MS, Jardiel T, Peiteado M, Mompean FJ, Hernandez MG, Garcia MA, Villegas M, Caballero AC. Intrinsic Compositional Inhomogeneities in Bulk Ti-Doped BiFeO<sub>3</sub>: Microstructure Development and Multiferroic Properties, Chem. Mater., 2013, 25: 1533–1541.
13. Mi JL, Jensen TN, Christensen M, Tyrsted C, Jørgensen JE, Iversen BB. High-Temperature and High-Pressure Aqueous Solution Formation, Growth, Crystal Structure, and Magnetic Properties of BiFeO<sub>3</sub>Nanocrystals, Chem.Mater., 2011, 23 : 1158–1165.
14. ParkTJ, Papaefthymiou GC, Viescas AJ, Moodenbaugh AR, Wong SS. Size-Dependent Magnetic Properties of Single-Crystalline Multiferroic BiFeO<sub>3</sub> Nanoparticles, Nano Lett. 2007, 7 : 766–772.

\*\*\*\*\*